

Bismuth-Assisted CdSe and CdTe Nanowire Growth on Plastics

Simon K. C. Lee,^{†,⊥} Yanghai Yu,[‡] Oscar Perez,[†] Sean Puscas,[†] Thomas H. Kosel,[§] and Masaru Kuno^{*,†}

[†]Department of Chemistry and Biochemistry and Notre Dame Radiation Laboratory, [‡]Department of Chemical Engineering, [§]Department of Electrical Engineering, University of Notre Dame, Notre Dame, Indiana, 46556, and [⊥]Nanotechnology Engineering, University of Waterloo, Waterloo, Ontario, Canada, N2L 3G1

Received July 7, 2009. Revised Manuscript Received September 1, 2009

A modified chemical vapor deposition process was used to synthesize long ($> 10\ \mu\text{m}$), 20–60 nm diameter CdSe and CdTe nanowires (NWs) at low temperatures on plastic. The approach applies synthetic strategies developed during the growth of solution-based semiconductor NWs. Namely, a thin Bi film is employed to induce NW growth at temperatures as low as $\sim 300\ ^\circ\text{C}$ on polyimide. This plastic is flexible, semitransparent, and possesses excellent chemical stability. Resulting wires have subsequently been characterized using various techniques, including scanning electron microscopy, transmission electron microscopy, and energy-dispersive X-ray spectroscopy. NW formation appears to follow a vapor–liquid–solid (VLS) mechanism with Bi nanoparticles inducing directional growth. The length, width, and overall density of the wires can be modified by varying the growth temperature, Bi film thickness, as well as the introduced precursor metal:chalcogen stoichiometry. Additional studies were conducted to grow wires on other substrates such as silicon, glass, indium–tin–oxide coated glass coverslips, and Teflon. This study highlights the ability to synthesize II–VI NWs at low temperatures on various materials including plastics and raises the possibility of eventually developing conformal NW solar cells.

Introduction

Semiconductor nanowires (NWs) have recently been applied toward proof-of-concept optical and electrical devices such as sensors,^{1,2} transistors,^{3,4} and photodetectors.^{5–7} These studies have primarily employed NWs synthesized via vapor–liquid–solid (VLS) growth. The process, with some notable exceptions,⁸ employs high temperatures ($T > 500\ ^\circ\text{C}$)⁹ and “catalyst” metal nanoparticles to induce the asymmetric growth of semiconductors on a substrate. Highly crystalline NWs result with diameters comparable to those of starting nanoparticles and with lengths exceeding $1\ \mu\text{m}$. Recent developments in the field have been summarized in refs 10 and 11.

At the same time, potential applications exist where it would be advantageous to directly grow NWs onto

substrates at low temperatures. For example, NWs could be grown onto existing electronic circuits or, alternatively, onto flexible conductive substrates for applications related to the development of conformal solar cells. Thus, interest exists in alternative, low temperature NW growth strategies.

In this study we demonstrate the low temperature growth of CdSe and CdTe NWs on a flexible plastic (polyimide) substrate. The approach is a modified chemical vapor deposition (CVD) process based on traditional VLS growth. While the choice of CdSe or CdTe is driven primarily by synthetic considerations, both materials are potential candidates for NW-based solar cells since their direct band gaps ($E_g = 1.74$ and $1.50\ \text{eV}$ at 300 K, respectively) correspond well to the solar spectrum. In this regard, previous studies have illustrated how CdSe or CdTe quantum dots (QDs)¹² and nanorods (NRs)^{13,14} can be employed in actual solar photovoltaics with significant ($\sim 3\%$) power conversion efficiencies when configured as Type-II heterojunctions.¹⁵

In what follows, we put our work into context by briefly outlining approaches for synthesizing NWs. Emphasis is placed on SLS and VLS growth. Namely, existing NW

*Corresponding author. E-mail: mkuno@nd.edu.

- (1) Wan, Q.; Li, Q. H.; Chen, Y. J.; Wang, T. H.; He, X. L.; Li, J. P.; Lin, C. L. *Appl. Phys. Lett.* **2004**, 84, 3654.
- (2) Zheng, G. F.; Patolsky, F.; Cui, Y.; Wang, W. U.; Lieber, C. M. *Nat. Biotechnol.* **2005**, 23, 1294.
- (3) Cui, Y.; Lieber, C. M. *Science* **2001**, 291, 851.
- (4) Huang, Y.; Duan, X. F.; Cui, Y.; Lauhon, L. J.; Kim, K. H.; Lieber, C. M. *Science* **2001**, 294, 1313.
- (5) Hayden, O.; Agarwal, R.; Lieber, C. M. *Nat. Mater.* **2006**, 5, 352.
- (6) Singh, A.; Li, X.; Protasenko, V.; Galantai, G.; Kuno, M.; Xing, H.; Jena, D. *Nano Lett.* **2007**, 7, 2999.
- (7) Yu, Y. H.; Protasenko, V.; Jena, D.; Xing, H. L.; Kuno, M. *Nano Lett.* **2008**, 8, 1352.
- (8) Wang, D. W.; Dai, H. J. *Angew. Chem., Int. Ed.* **2002**, 41, 4783.
- (9) Wu, Y. Y.; Fan, R.; Yang, P. D. *Nano Lett.* **2002**, 2, 83.
- (10) Lu, W.; Lieber, C. M. *J. Phys. D: Appl. Phys.* **2006**, 39, R387.
- (11) Law, M.; Goldberger, J.; Yang, P. D. *Annu. Rev. Mater. Res.* **2004**, 34, 83.

- (12) Robel, I.; Subramanian, V.; Kuno, M.; Kamat, P. V. *J. Am. Chem. Soc.* **2006**, 128, 2385.
- (13) Sun, B. Q.; Marx, E.; Greenham, N. C. *Nano Lett.* **2003**, 3, 961.
- (14) Huynh, W. U.; Dittmer, J. J.; Alivisatos, A. P. *Science* **2002**, 295, 2425.
- (15) Gur, I.; Fromer, N. A.; Geier, M. L.; Alivisatos, A. P. *Science* **2005**, 310, 462.

growth methodologies include template approaches¹⁶ as well as solution-based methods such as oriented attachment,¹⁷ solution–liquid–solid (SLS),^{18,19} and supercritical–fluid–liquid–solid (SFLS)²⁰ growth. More common approaches include thermal evaporation,²¹ laser ablation,^{22,23} and VLS⁹ growth.

In the latter VLS mechanism, an inert carrier gas transports vapor phase precursors into a heated reactor. As originally proposed by Wagner and Ellis,²⁴ whisker growth is aided by the presence of a molten metal catalyst, containing elements derived from vapor phase precursors. When particle saturation occurs, the desired semiconductor nucleates and precipitates at the liquid catalyst/solid substrate interface. Continued addition of material at this junction then leads to directional semiconductor growth. The use of nanometer-sized metal catalyst droplets ensures NW formation since a direct proportionality exists between starting nanoparticle (NP) diameters and those of resulting wires.²⁵ This application of molten, nanometer-sized metal catalysts is also common to SLS growth.^{18,19}

In this regard, the primary feature distinguishing SLS from VLS growth is the use of catalyst particles with melting points suitable for solution chemistry. Namely, elements such as In ($T_m = 157^\circ\text{C}$),²⁶ Sn ($T_m = 232^\circ\text{C}$),²⁷ Bi ($T_m = 271^\circ\text{C}$), and Pb ($T_m = 328^\circ\text{C}$)²⁸ are often used over Au ($T_m = 1064^\circ\text{C}$) which is a common VLS catalyst. A number of solution-based reactions have therefore focused on Bi or Au/Bi core/shell NPs to induce NW

growth within the following semiconductor families: Group IV: Si,²⁹ Ge,³⁰ Group II–VI: ZnTe,¹⁹ CdS,³¹ CdSe,^{32–35} CdTe,^{36,37} Group III–V: InP,^{38,39} InAs,^{38,40} GaP,³⁸ and GaAs,⁴¹ Group IV–VI: PbS,⁴² and PbSe.⁴³

This realization that Bi promotes low temperature NW growth in a variety of systems has motivated extensions of these studies. For example, Ouyang and Park have synthesized CdS/CdSe NW heterostructures directly onto Bi-coated silicon and III–V substrates in solution.⁴⁴ The approach has also been used by Dorn and Bawendi to generate substrate-localized CdSe NWs, employing an external electric field to aid their growth.⁴⁵ Likewise, short CdTe NRs have been synthesized onto Bi-coated sapphire by laser ablation.⁴⁶

In this study, we employ thin Bi films to promote CdSe and CdTe NW growth on flexible plastic substrates. This is motivated by potential uses of such NWs in applications where conformal properties would be advantageous. An example entails constructing flexible, NW-based solar cells. Furthermore, the ability to synthesize semiconductor NWs directly onto such substrates at low temperatures may have other applications that we do not yet foresee.

Experimental Section

Materials. Hexane, acetone, and toluene were purchased and used as received from Fisher Scientific. Dimethylcadmium (CdMe_2 , Strem) was filtered through a $0.2\ \mu\text{m}$ PTFE syringe filter in a nitrogen-filled glovebox and was stored in a freezer. Bis(trimethylsilyl)selenide $[(\text{TMS})_2\text{Se}$, Gelest] and bis(trimethylsilyl)telluride $[(\text{TMS})_2\text{Te}$, Acros] were used as received and were also stored in a glovebox freezer. Bismuth pellets ($\geq 99.99\%$) and indium wire ($\geq 99.99\%$) were purchased from Alfa Aesar. Indium–tin–oxide (ITO) coated glass coverslips were purchased from SPI Supplies. Silicon wafers were purchased from MEMC Electronic Materials. Polyimide sheets were donated by Dupont.

Thin Film Formation. All substrates were sonicated in acetone for 5 min prior to use. Bismuth or indium was evaporated onto substrates using a thermal evaporator (Ladd). Film thicknesses were monitored using a quartz crystal microbalance (Sycon).

CdSe/CdTe Nanowire Synthesis. Substrates were placed atop a holder situated at the center of a single zone ceramic tube furnace. The unit was then heated, and the substrate's temperature was monitored using a thermocouple attached directly to the holder. In parallel, two 10 mL solutions, consisting of CdMe_2 in hexane and $(\text{TMS})_2\text{Se}$ [or $(\text{TMS})_2\text{Te}$] in hexane, were prepared under nitrogen in a glovebox.

Various metal:chalcogen mole ratios were employed during these reactions. Stoichiometric 1:1 metal:chalcogen mole ratio solutions were prepared for CdSe reactions by adding $12\ \mu\text{L}$

- (16) Hurst, S. J.; Payne, E. K.; Qin, L. D.; Mirkin, C. A. *Angew. Chem., Int. Ed.* **2006**, *45*, 2672.
- (17) Tang, Z. Y.; Kotov, N. A.; Giersig, M. *Science* **2002**, *297*, 237.
- (18) Kuno, M. *Phys. Chem. Chem. Phys.* **2008**, *10*, 620.
- (19) Wang, F. D.; Dong, A. G.; Sun, J. W.; Tang, R.; Yu, H.; Buhro, W. E. *Inorg. Chem.* **2006**, *45*, 7511.
- (20) Holmes, J. D.; Johnston, K. P.; Doty, R. C.; Korgel, B. A. *Science* **2000**, *287*, 1471.
- (21) Ma, C.; Wang, Z. L. *Adv. Mater.* **2005**, *17*, 2635.
- (22) Morales, A. M.; Lieber, C. M. *Science* **1998**, *279*, 208.
- (23) Zhang, Y. F.; Tang, Y. H.; Wang, N.; Yu, D. P.; Lee, C. S.; Bello, I.; Lee, S. T. *Appl. Phys. Lett.* **1998**, *72*, 1835.
- (24) Wagner, R. S.; Ellis, W. C. *Appl. Phys. Lett.* **1964**, *4*, 89.
- (25) Gudiksen, M. S.; Wang, J. F.; Lieber, C. M. *J. Phys. Chem. B* **2001**, *105*, 4062.
- (26) Iacopi, F.; Vereecken, P. M.; Schaekers, M.; Caymax, M.; Moelans, N.; Blanpain, B.; Richard, O.; Detavernier, C.; Griffiths, H. *Nanotechnology* **2007**, *18*, 505307.
- (27) Gao, P. X.; Ding, Y.; Wang, I. L. *Nano Lett.* **2003**, *3*, 1315.
- (28) Bierman, M. J.; Lau, Y. K. A.; Jin, S. *Nano Lett.* **2007**, *7*, 2907.
- (29) Heitsch, A. T.; Fanfair, D. D.; Tuan, H. Y.; Korgel, B. A. *J. Am. Chem. Soc.* **2008**, *130*, 5436.
- (30) Lu, X. M.; Fanfair, D. D.; Johnston, K. P.; Korgel, B. A. *J. Am. Chem. Soc.* **2005**, *127*, 15718.
- (31) Puthussery, J.; Lan, A. D.; Kosel, T. H.; Kuno, M. *ACS Nano* **2008**, *2*, 357.
- (32) Yu, H.; Li, J. B.; Loomis, R. A.; Gibbons, P. C.; Wang, L. W.; Buhro, W. E. *J. Am. Chem. Soc.* **2003**, *125*, 16168.
- (33) Grebinski, J. W.; Hull, K. L.; Zhang, J.; Kosel, T. H.; Kuno, M. *Chem. Mater.* **2004**, *16*, 5260.
- (34) Li, Z.; Kornowski, A.; Myalitsin, A.; Mews, A. *Small* **2008**, *4*, 1698.
- (35) Wang, F. D.; Tang, R.; Kao, J. L. F.; Dingman, S. D.; Buhro, W. E. *J. Am. Chem. Soc.* **2009**, *131*, 4983.
- (36) Kuno, M.; Ahmad, O.; Protasenko, V.; Bacinello, D.; Kosel, T. H. *Chem. Mater.* **2006**, *18*, 5722.
- (37) Sun, J. W.; Wang, L. W.; Buhro, W. E. *J. Am. Chem. Soc.* **2008**, *130*, 7997.
- (38) Fanfair, D. D.; Korgel, B. A. *Cryst. Growth. Des.* **2005**, *5*, 1971.
- (39) Wang, F. D.; Yu, H.; Li, J. B.; Hang, Q. L.; Zemlyanov, D.; Gibbons, P. C.; Wang, L. W.; Janes, D. B.; Buhro, W. E. *J. Am. Chem. Soc.* **2007**, *129*, 14327.

- (40) Wang, F. D.; Yu, H.; Jeong, S.; Pietryga, J. M.; Hollingsworth, J. A.; Gibbons, P. C.; Buhro, W. E. *ACS Nano* **2008**, *2*, 1903.
- (41) Dong, A.; Yu, H.; Wang, F.; Buhro, W. E. *J. Am. Chem. Soc.* **2008**, *130*, 5954.
- (42) Sun, J. W.; Buhro, W. E. *Angew. Chem., Int. Ed.* **2008**, *47*, 3215.
- (43) Hull, K. L.; Grebinski, J. W.; Zhang, J.; Kosel, T. H.; Kuno, M. *Chem. Mater.* **2005**, *17*, 4416.
- (44) Ouyang, L.; Maher, K. N.; Yu, C. L.; McCarty, J.; Park, H. *J. Am. Chem. Soc.* **2007**, *129*, 133.
- (45) Dorn, A.; Wong, C. R.; Bawendi, M. G. *Adv. Mater.* **2009**, *21*, 1.
- (46) Neretina, S.; Hughes, R. A.; Britten, J. F.; Sochinskii, N. V.; Preston, J. S.; Mascher, P. *Nanotechnology* **2007**, *18*, 275301.

(167 μmol) of CdMe_2 and 42 μL (167 μmol) of $(\text{TMS})_2\text{Se}$ each to 10 mL hexane. Analogous 2:1 metal:chalcogen solutions were prepared for CdTe reactions by adding 24 μL (332 μmol) of CdMe_2 and 47 μL (166 μmol) of $(\text{TMS})_2\text{Te}$ each to 10 mL hexane. To prevent Te from precipitating due to exposure to light and air, $(\text{TMS})_2\text{Te}$ solutions were stored in N_2 -filled containers covered by aluminum foil prior to use.

When a desired substrate temperature was reached, both metal:chalcogen solutions were added to two bubblers connected to the tube furnace and were subsequently introduced by passing nitrogen through them. The N_2 flow rate was set to 200 cc/min. Following addition, the reaction was left to run for approximately 45 min until the bubblers were completely dry. At this point, the reactor was allowed to cool under nitrogen for 30 min. Substrates were then removed and were stored in airtight containers for further analysis.

Control experiments were conducted by omitting Bi films from substrates. NW growth was then attempted with these “blanks”. In no case were wires observed, regardless of reaction condition. This indicates the necessity of Bi for NW production. Furthermore, bulk CdSe powder was also tested as a potential precursor by adding 10 mg (52.3 μmol) to a crucible and loading it into the reactor. The system was then heated to 400 $^\circ\text{C}$ and was left at this temperature for 45 min prior to cooling. Again, no CdSe NWs were obtained under these conditions. Lastly, to test the impact of reaction time, a typical (optimized) reaction was stopped after 20 min and was allowed to cool. Although NWs were obtained, they were found to be shorter than wires grown for the full 45 min duration of a typical reaction.

Characterization. Resulting samples were primarily characterized using scanning electron microscopy (SEM) and transmission electron microscopy (TEM). To prepare samples for SEM experiments, approximately 5 nm of chromium was deposited onto specimens using a sputter coater (Emitech). SEM studies were conducted using a Hitachi S-4500 field emission scanning electron microscope. Energy-dispersive X-ray spectroscopy (EDXS) experiments were also carried out using both SEM-based (4pi) and TEM-based (Thermo) EDXS attachments.

TEM specimens were prepared by first sonicating NW-coated substrates in toluene. Resulting NW suspensions were then dropcast onto ultrathin carbon-coated TEM grids (Ladd) and were allowed to dry. Preliminary low resolution TEM imaging was conducted with a JEOL 100SX instrument. Both low and high resolution TEM micrographs as well as selected area diffraction patterns were taken with a JEOL 2010 LaB₆ TEM. NW diameters were determined by measuring over 100 wires within a given ensemble.

Optical Studies. Linear extinction measurements were conducted with a Cary 50 Bio UV/Visible spectrometer. Photoluminescence experiments were carried out using a home-built microscope system based on a Nikon TE2000U frame and capable of single molecule imaging. NWs were excited using the 473 nm output of a CW diode laser (Oxxus). Detected emission was then imaged with a Peltier cooled CCD (DVC). More information about the apparatus can be found in ref 47. Incident photon to carrier conversion efficiencies and photocurrent action spectra were obtained separately using a different home-built microscope described in more detail in ref 7. To construct rudimentary photoelectrochemical solar cells, NWs were grown directly onto ITO-coated glass coverslips. A 0.05 M

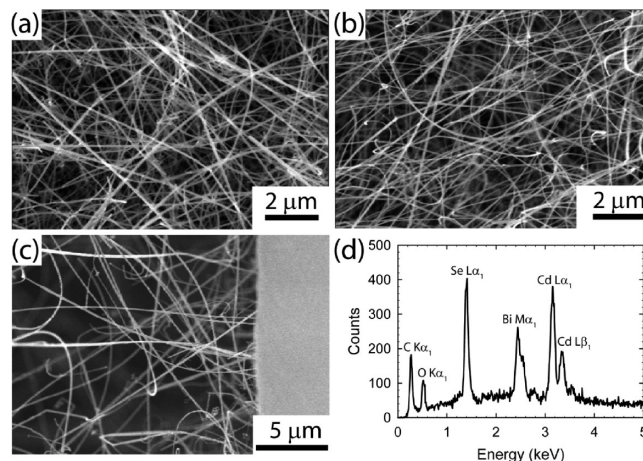


Figure 1. (a,b) Representative SEM micrographs of CdSe NW ensembles grown on polyimide at 400 $^\circ\text{C}$. (c) Cross-sectional view of the polyimide substrate with CdSe NWs grown onto it; (d) SEM-based EDXS spectrum of a CdSe NW ensemble on polyimide, showing its elemental composition: Cd : 52.07%, Se : 49.73% ($\sigma = 1.73$). The C and O peaks are thought to be predominantly polyimide related while the Bi peak likely stems from surface localized Bi .

Na_2S solution was then used as a redox couple along with Pt foil as a counter electrode. Samples were subsequently excited using the grating dispersed output of a supercontinuum white light source (Fianium).

Results and Discussion

Given prior successes using Bi to induce the solution-phase growth of NWs, we were interested in investigating whether it could also be used to produce wires at low temperatures on plastic through VLS growth. CdSe and CdTe were therefore chosen as candidate materials given that we and others have previously shown that Bi readily promotes their directional crystallization in SLS preparations.^{32–37} Furthermore, these materials have been used in QD/NR-based photovoltaics and, as a consequence, may have potential uses in NW-based solar cells.

Figure 1a and b show representative SEM images of CdSe NWs grown on polyimide at 400 $^\circ\text{C}$. The micrographs reveal that NW growth can indeed be induced on these flexible substrates. A cross-sectional SEM image of CdSe NWs on polyimide is shown in Figure 1c, highlighting NW attachment to the substrate. A detailed inspection of all micrographs indicates that obtained wire diameters are much larger than those seen in counterpart SLS specimens. Namely, analyses of these ensembles show wire diameters on the order of 20–50 nm, whereas lengths readily exceed 10 μm . By contrast, solution-based CdSe NWs made using either ~ 2 –3 nm diameter Bi NPs,^{33,48} or Bi alone,⁴⁹ have mean diameters between 5 and 12 nm. Corresponding ensemble diameter distributions are on the order of 20–35% and are comparable to but somewhat larger than those in SLS preparations (15–30%).³³

(47) Protasenko, V. V.; Hull, K. L.; Kuno, M. *Adv. Mater.* **2005**, *17*, 2942.

(48) Grebinski, J. W.; Richter, K. L.; Zhang, J.; Kosel, T. H.; Kuno, M. *J. Phys. Chem. B* **2004**, *108*, 9745.

(49) Puthussery, J.; Kosel, T. H.; Kuno, M. *Small* **2009**, *5*, 1112.

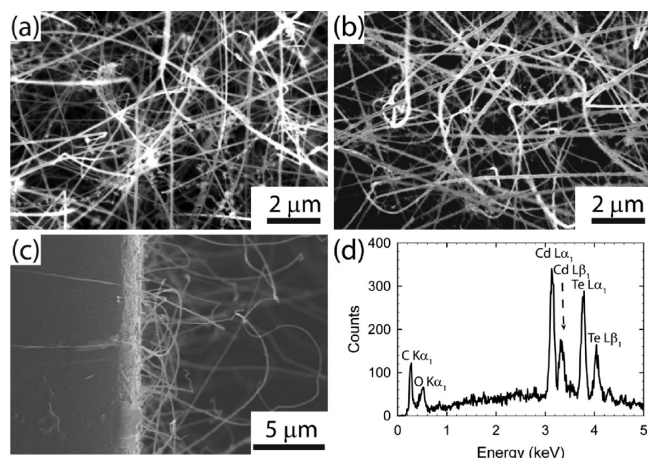


Figure 2. (a,b) Representative SEM micrographs of CdTe NW ensembles grown on polyimide at 400 °C. (c) Cross-sectional view of the polyimide substrate with CdTe NWs grown onto it; (d) SEM-based EDXS spectrum of a CdTe NW ensemble on polyimide, showing its elemental composition: Cd: 52.69%, Te: 47.31% ($\sigma = 3.83$). The C and O peaks are thought to be predominantly polyimide related.

By varying the identity of the chalcogen precursor, namely from $(\text{TMS})_2\text{Se}$ to $(\text{TMS})_2\text{Te}$, CdTe NWs could also be obtained on polyimide. Figure 2a and b show representative SEM micrographs of such ensembles grown at 400 °C. The corresponding SEM cross-sectional view (Figure 2c) also demonstrates that NWs adhere to the substrate. As with prior CdSe NWs, obtained CdTe diameters appear larger than those of comparable wires made using solution chemistry.^{36,37} Mean CdTe NW diameters range from 30 to 70 nm, whereas those of the SLS wires vary between 8 and 10 nm. Ensemble diameter distributions are also somewhat larger and range from 25 to 30%. In either case, elemental analysis confirms their composition as demonstrated in Figure 2d. For either CdSe or CdTe, additional single NW, TEM-based elemental analyses (Supporting Information (SI) Figure S1) confirm conclusions from (ensemble) EDXS measurements. Color photographs of the resulting NW specimens are shown in SI Figure S2.

Growth Parameters. To optimize NW growth, various reaction parameters were altered. Specifically, we varied the growth temperature, Bi film thickness, metal:chalcogen mole ratio, and identity of the low melting metal “catalyst”. Comparisons to solution-based NW growth could therefore be made, allowing points of commonality to be identified. In all cases, polyimide was chosen as a flexible plastic substrate since it was readily available, possessed a relatively high melting threshold ($T_m \sim 360\text{--}410$ °C) and was also chemically stable. An additional study was conducted to investigate NW growth on other substrates such as glass, indium–tin–oxide and Teflon.

Growth Temperature. The key motivation of this study was to investigate upper and lower temperature bounds for NW growth on polyimide and to see whether resulting wires were crystalline. We note that analogous solution-based NWs are highly crystalline despite low (~ 300 °C) growth temperatures.^{29–43} This might then

imply highly crystalline wires resulting from our CVD studies.

CdSe and CdTe NWs were therefore synthesized on polyimide at temperatures between 300 and 430 °C, using thin bismuth films. Temperatures above 430 °C yielded NWs but led to polyimide substrates becoming brittle after cooling, making them prone to shattering. By contrast, temperatures below 300 °C did not generally promote NW growth.

An exception to this was the use of ~ 3 nm diameter Au/Bi NPs⁴⁸ which yielded CdSe NWs on silicon at 250 °C. In this case, NPs were dropcast directly onto substrates prior to inserting them into the tube furnace. Although NWs were obtained, resulting surface coverages were often sparse, leading us to forego this approach in favor of the above Bi thin film procedure. A SEM micrograph of such Au/Bi–catalyzed NWs grown at 250 °C can be found in SI Figure S3.

Notably, CVD reaction temperatures are slightly higher than those of previous CdSe^{32–35} ($T = 250\text{--}350$ °C) and CdTe^{36,37} ($T = 220\text{--}285$ °C) SLS reactions. At the lower end of the employed temperature range (300–430 °C), occasional NW branching³³ was seen in resulting ensembles. However, such samples contained a wide variety of ill-defined NW morphologies with relatively sparse surface coverages, short NW lengths (< 2 μm) and with diameters that tapered toward one end. By contrast, reactions at temperatures above ~ 370 °C yielded predominantly straight NWs, which were long (> 10 μm) and which possessed relatively uniform dimensions. As a consequence, CVD reactions were optimized in this temperature regime.

High resolution TEM micrographs (HRTEMs) of resulting CdSe and CdTe NWs are shown in Figure 3. Specifically, Figure 3a and b illustrate high resolution micrographs of CdSe wires grown on polyimide at 400 °C. NWs are approximately 27 nm in diameter with accompanying width distributions of $\sim 23\%$. Complementary HRTEM micrographs of analogous CdTe NWs grown on polyimide at 400 °C are also shown in Figures 3c and d. In both cases, insets show selected area electron diffraction (SAED) patterns of representative wires. Both HRTEM and SAED images show that the produced CdSe and CdTe NWs are predominantly polycrystalline. This is unlike the case of solution-based CdSe and CdTe NWs which are highly crystalline despite their low growth temperatures. Additional low and high resolution images of these wires can be found in SI Figures S4 and S5.

Of note in either case is the appearance of occasional narrow diameter NWs with widths on the order of 10–20 nm. Their presence suggests that the vapor phase approach can produce wires with comparable dimensions to those from SLS preparations. However, despite numerous attempts, we were not able to identify critical parameters defining this growth regime.

At the same time, we find that a smaller subset of crystalline CdO wires exists within these ensembles. They tend to be more apparent in CdSe than in CdTe. Figure 3e and f shows representative HRTEM images of these

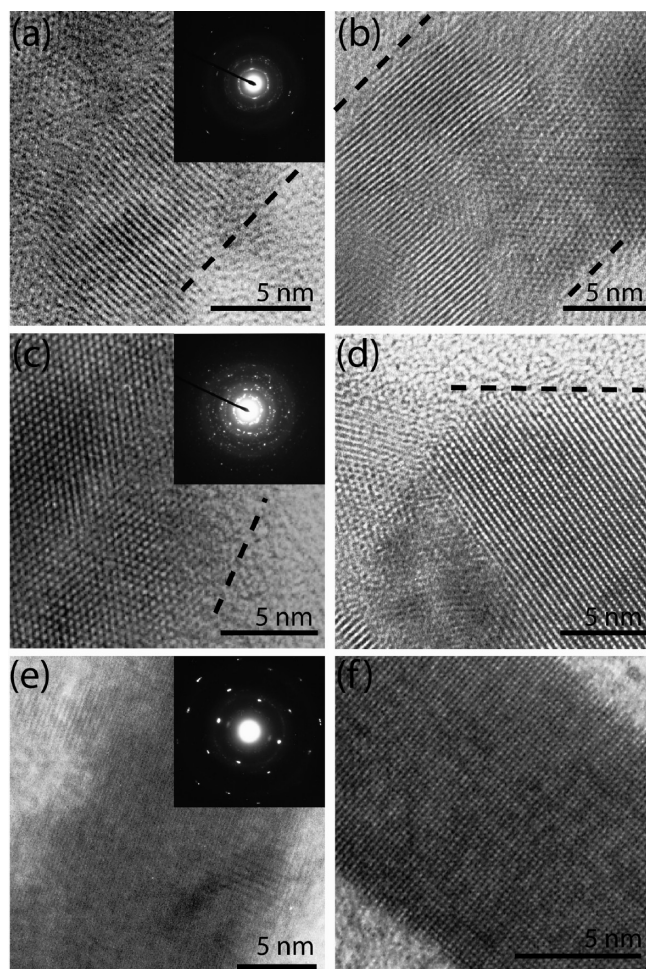


Figure 3. HRTEM micrographs of (a, b) CdSe, (c, d) CdTe, and (e, f) CdO NWs grown on polyimide at 400 °C. Insets correspond to selected area diffraction patterns from representative NWs.

wires, which possess $\langle 100 \rangle$ growth directions. A corresponding SAED image has also been included as an inset. We suspect that such wires may result from the presence of residual oxygen in the system, despite the continuous flow of N_2 during the reaction. Although quantifying their representation within an actual ensemble is difficult, visual inspection and accompanying EDXS analyses of individual wires suggest that they are not the majority species in either CdSe or CdTe ensembles. This is corroborated by the near stoichiometric (ensemble) EDXS spectra of CdSe and CdTe samples, shown in Figures 1d and 2d.

Bi Film Thickness. Bi film thicknesses directly impact resulting NW diameters. Namely, thicker films yield larger diameter wires. To illustrate, at 400 °C, a 10 nm Bi film produces CdSe ensembles with mean widths on the order of ~ 30 nm. By contrast, thinner (5 nm) films produce wires with average diameters on the order of ~ 20 nm. However, the diameter distribution becomes wider and increases from $\sim 23\%$ in the former case to $\sim 30\%$ in the latter. An identical trend can be seen in CdTe wires and similar sizing observations have been reported by Ouyang and Park.⁴⁴

We interpret Bi thickness-dependent diameters as the result of thicker Bi films leading to larger NP droplets

when molten. This is corroborated by extensive studies from Olson and Allen⁵⁰ who have shown that Bi NP size variations originate from thickness-dependent gaps between “islands” formed during heating. The smaller frequency of these gaps in thicker films leads to larger islands, which in turn, result in larger NPs. The direct relationship between catalyst film thickness⁵¹ (or droplet size¹⁹) and NW diameter then results in large diameter NWs. This behavior holds at the opposite limit and, as such, thinner Bi films yield correspondingly thinner wires. As an independent control experiment, we therefore tested this trend by annealing a bismuth covered polyimide substrate at 400 °C under forming gas and find that thicker films produce larger particles upon melting. This is illustrated in the Supporting Information where Figure S6 qualitatively demonstrates that 100, 50, and 10 nm Bi films melt to yield successively smaller particles.

An additional influence of the Bi film thickness is the apparent smoothness of resulting NWs. Namely, when thick (> 20 nm) Bi films are used, not only are resulting wires thicker but they are also rougher. By contrast, thinner films (< 10 nm) lead to wires with relatively smooth surfaces. The effect is illustrated in the SI through representative SEM micrographs (Figures S7–S9). In either case, we speculate that this may stem from catalyst material diffusing toward the substrate during NW formation.⁵² This would then induce subsequent radial growth, which if uneven would lead to rough NW surfaces. Further studies, however, are needed to verify this hypothesis.

Metal to Chalcogen Mole Ratio. As with temperature and Bi film thickness, the metal to chalcogen mole ratio significantly influences NW growth. Namely, raising this value above 3:1 increases the resulting NW diameter, reduces its length and leads to ill-defined morphologies. To maximize the synthesis of thin CdSe or CdTe NWs, the ratio was therefore kept as low as possible. However, values of 1:3 did not promote CdSe or CdTe growth. Thus metal:chalcogen mole ratios were varied empirically between these two limits to optimize their production.

In the case of CdSe, a 1:1 ratio worked best, whereas a 2:1 ratio was preferred for synthesizing CdTe NWs (SI Figure S10). Samples made using these values demonstrated the narrowest diameters, longest lengths, and largest growth densities on polyimide. Despite slight asymmetries in the introduced precursor stoichiometries, ensemble and single wire EDXS measurements confirm near stoichiometric 1:1 metal:chalcogen mole ratios in both cases (Figures 1d, 2d, and S1 of the SI).

Interestingly, differences exist between the optimal metal:chalcogen stoichiometries described here and those of prior solution-based syntheses. Namely, SLS CdSe, and CdTe NWs utilize optimal metal:chalcogen ratios

(50) Olson, E. A.; Efremov, M. Y.; Zhang, M.; Zhang, Z.; Allen, L. H. *J. Appl. Phys.* **2005**, *97*, 9.

(51) Huang, M. H.; Wu, Y. Y.; Feick, H.; Tran, N.; Weber, E.; Yang, P. D. *Adv. Mater.* **2001**, *13*, 113.

(52) Dick, K. A.; Deppert, K.; Samuelson, L.; Wallenberg, L. R.; Ross, F. M. *Nano Lett.* **2008**, *8*, 4087.

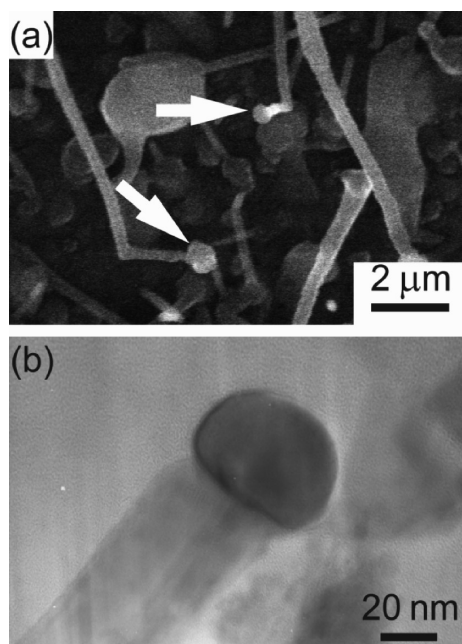


Figure 4. (a) SEM and (b) TEM micrographs illustrating catalyst particles at the tip of growing NWs.

of 7:1³³ and 6:1.³⁶ By contrast, more stoichiometric 1:1 (CdSe) and 2:1 (CdTe) values are used here.

Metal Catalyst Identity. To see whether NWs could be synthesized at temperatures significantly below 300 °C, additional growth studies were conducted using In thin films. Bulk In has a melting point of 157 °C and can, in principle, support low temperature NW growth. Indium-catalyzed growth studies were therefore conducted by depositing ~10 nm of In onto polyimide.

However, under the same conditions used in optimized Bi preparations, no NW growth was observed. Additional experiments, altering growth parameters such as the metal to chalcogen mole ratio, film thickness and growth temperature, were also conducted but likewise did not produce NWs. In most cases, only In nanoparticles were observed. The reason for this lack of reactivity is unclear although it could stem from issues related to the solubility of Cd or Se (Te) in In. In this respect, it is notable that few studies^{26,53} have employed In as a low melting catalyst to promote NW growth.

NW Growth Mechanism. In all cases, we posit that NW growth occurs through a VLS mechanism. Namely, Bi NP formation induces the asymmetric crystallization of NWs on employed substrates. This hypothesis has been supported by SEM observations of Bi particles attached to NW ends as shown in Figure 4a. A corresponding EDXS spectrum of a given Bi NP is also illustrated in SI Figure S11. However, finding instances of such particles attached to NW ends is often difficult for reasons that are not completely clear. A potential explanation for this involves catalyst diffusion from the NW tip to the substrate during growth, as mentioned earlier. This phenomenon has recently been reported in Au-catalyzed

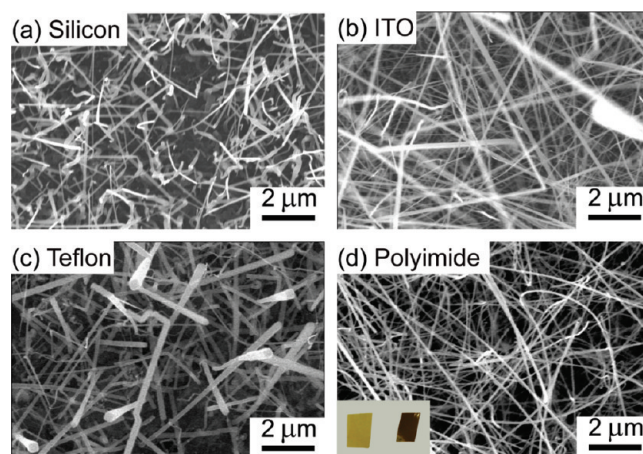


Figure 5. SEM micrographs of CdSe NWs grown on (a) silicon, (b) ITO coated glass coverslips, (c) Teflon, and (d) polyimide. Inset: (d) color photograph of the polyimide substrate before (left) and after (right) NW growth.

Si NWs⁵² and appears consistent with the difficulties experienced here.

Similar problems seeing Bi NPs attached to NW ends exist in TEM experiments although instances such as Figure 4b can be found. We speculate that in these latter experiments any remaining catalyst particles on the wires may have further detached themselves during sample preparation. In this regard, TEM specimens are prepared by sonicating NWs off the polyimide substrate (see the Experimental Section). This hypothesis is supported by observed instances of blunt NW ends where it appears that a particle might have once resided. Identical observations have been made with solution-based NWs and have been similarly explained as catalyst NPs falling off wires during post synthesis processing.^{33,36}

Substrate Identity. As an additional study, we investigated whether NWs could be produced on substrates other than polyimide. NW growth was therefore attempted on glass, indium–tin–oxide (ITO) coated glass coverslips, silicon and Teflon. In all cases, Bi thin films were used to promote NW growth. Figure 5 shows representative SEM micrographs of wires produced on silicon (Figure 5a), ITO (Figure 5b), and Teflon (Figure 5c). A polyimide sample is shown in Figure 5d for comparison purposes. Apparent NW growth can be seen in all cases.

Note that comprehensive studies were not conducted to optimize NW growth on these alternative substrates as we were primarily interested in wire growth on polyimide. We did notice, however, that under identical conditions as optimized polyimide reactions, resulting NWs on ITO, silicon and Teflon did not appear to possess comparable qualities in terms of NW length, diameter, and growth density. This may suggest additional substrate influences, such as variations in surface temperature and degree of catalyst diffusion to the substrate,⁵² which would, in turn, lead to differences in NW size, shape, and morphology.

Preliminary Optical Studies and Applications. Resulting CdSe NWs were investigated optically to better characterize their properties. For these measurements, samples

(53) Yu, H.; Buhro, W. E. *Adv. Mater.* **2003**, *15*, 416.

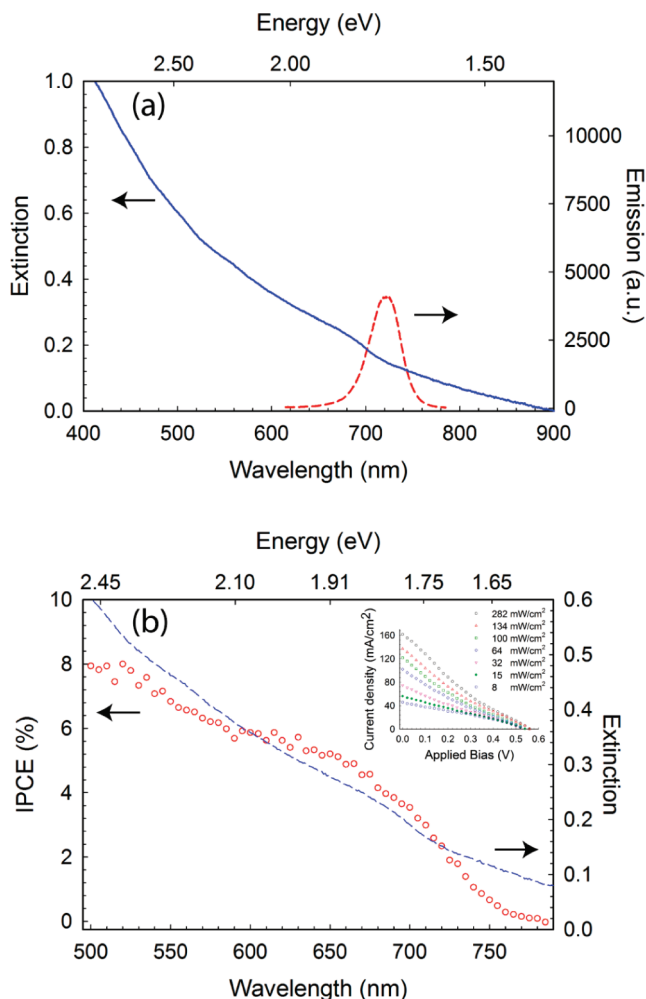


Figure 6. (a) Extinction (solid blue line) and photoluminescence (dashed red line) of a CdSe NW ensemble synthesized directly onto a glass coverslip. (b) Extinction (dashed blue line) and incident photon to carrier conversion efficiency (red circles) of CdSe NWs across the visible.

were prepared by directly synthesizing NWs onto glass microscope coverslips under the optimized conditions described above. Figure 6a shows a representative extinction spectrum (average NW diameter = 28 nm, $\sigma = \sim 23\%$). Apparent is an absorption onset around 685 nm (1.81 eV), consistent with prior linear absorption measurements of CdSe NWs.^{32,48,49} However, a significant scattering background makes determining the actual peak position of their band edge absorption difficult. This scattering contribution to the extinction can be seen through a prominent tail in the spectrum that extends to the red beyond 700 nm. The photoluminescence (PL) signal of the sample is also shown and appears to be band edge in nature. However, corresponding quantum yields are low and lie below 0.1%, based on a comparison to the emission of individual solution-based CdSe NWs.⁴⁷

Such QY comparisons were made by first estimating the absorption cross section of an individual solution-based CdSe NW. Various procedures exist for doing this

and can be found in refs 47, 54, and 55. Thus at a given excitation intensity, the number of absorbed photons could be determined. Then, given the collection efficiency of our microscope ($\sim 5\%$)⁴⁷ as well as the measured count rate on a single photon counting avalanche photodiode, the number of photons emitted by the wire could be determined. A representative solution-based NW QY of $\sim 0.1\%$ was obtained as the ratio of emitted to absorbed photons. Subsequent sample-to-sample QY estimates were then based on brightness differences between CVD-based and solution-based wires when imaged on a CCD camera, taking into account differences in their respective absorption cross sections.

Finally, to test the applicability of these NWs for solar cell applications, preliminary proof-of-concept NW photoelectrochemical cells were prepared. Specifically, CdSe NWs were grown directly onto ITO-coated glass coverslips. A Na_2S redox couple (0.05 M) was then added to the sample along with a platinum counter electrode to complete the photoelectrochemical cell. Devices were illuminated with visible light using the tunable output of a grating dispersed supercontinuum white light source, and incident photon to carrier conversion efficiencies (IPCE) were measured across the visible. Figure 6b plots these values against excitation wavelength and show numbers that vary from 1 to 8%. More importantly, the resulting action spectrum closely resembles the extinction spectrum of the wires, indicating that they are responsible for the photoresponse.

Subsequent I–V measurements under simulated AM 1.5, 1 sun (100 mW/cm^2) conditions yield a representative open circuit voltage of $V_{oc} = 0.54 \text{ V}$ and a short circuit current density of $121.63 \mu\text{A/cm}^2$ (inset, Figure 6b). A corresponding fill factor is $FF = 0.20$ with an associated power conversion efficiency of $\sim 0.013\%$. A table of relevant parameters under other excitation intensities can be found in the SI. Although the latter conversion efficiency is low, this proof-of-principle demonstration suggests that the wires may ultimately have photovoltaic applications, and further studies into their limiting constraints are needed.

Conclusions

Using a modified CVD technique, employing a Bi catalyst important to the solution-phase growth of 1D nanostructures, CdSe and CdTe NWs were produced on flexible plastic substrates. Specifically, a low melting Bi thin film was used to promote NW growth directly onto polyimide at temperatures as low as 300°C . The method was also successful in producing NWs on other substrates such as silicon, glass, indium–tin–oxide (ITO) coated glass coverslips, and Teflon.

Resulting NWs appear to grow through a VLS mechanism. Namely, heating the substrate melts the Bi film and eventually leads to the formation of nanometer-sized Bi droplets. These molten NPs then solubilize elements from the pyrolysis of gas phase precursors. Subsequent

(54) Protasenko, V.; Bacinello, D.; Kuno, M. *J. Phys. Chem. B* **2006**, *110*, 25322.

(55) Giblin, J. P.; Protasenko, V.; Kuno, M. *ACS Nano* **2009**, *3*, 1979.

saturation followed by nucleation results in NW growth at the catalyst/substrate interface.

HRTEM micrographs suggest that the wires are polycrystalline and have diameters between 20 and 60 nm. Accompanying lengths exceed 10 μm . Corresponding surface coverages are high and, as such, may be of practical interest. In this regard, our current synthetic and optical studies suggest that future investigations may lead to the efficient, low temperature, production of NWs on other flexible/conductive substrates, which may in turn, enable the development of conformal NW solar cells.

Acknowledgment. We thank Caitlin Trombly for early contributions to this study and Jay Giblin for assisting in the extinction and emission measurements. M.K. thanks the Notre Dame Energy Center for financial support of this work. M.K. also thanks the NSF CAREER program (CHE-0547784), the Notre Dame Radiation Laboratory, and the

DOE Office of Basic Energy Sciences for partial financial support as well as access to their equipment and facilities. M.K. is a Cottrell Scholar of Research Corporation. S.K.C.L. and Y.Y. contributed equally to this study.

Supporting Information Available: Elemental analysis and stoichiometry of single CdSe and CdTe NWs. Color photographs of resulting NW-coated polyimide substrates. SEM micrograph of Au/Bi catalyzed NWs on silicon. Low resolution TEM micrographs of CdSe and CdTe NWs. High resolution TEM micrographs of CdSe and CdTe NWs. SEM images of bismuth particles formed after melting Bi films on polyimide. SEM micrographs of NWs synthesized with varying Bi film thickness, metal:chalcogen mole ratio as well as examples of smooth and rough NWs. EDXS spectrum of a catalyst particle. Table of NW photoelectrochemical solar cell parameters. This material is available free of charge via the Internet at <http://pubs.acs.org>.